REVIEW ARTICLE Indian Journal of Agricultural Research, Volume 60 Issue 11: 1639-1654 (November 2026)

Hyperspectral Imaging for Disease Detection in Wheat Crops: A Comprehensive Survey

M. Deepak[1], Gopal K. Shyam[2]

10.18805/IJARe.A-6533

ABSTRACT

Hyperspectral imaging (HSI) has emerged as a game-changing technology for precision agriculture because it captures detailed spectral signatures over hundreds of finely-resolved, continuous wavelength bands. This feature makes possible a detailed description of species-specific plant physiological states to enable early, precise and non-destructive identification of diseases in crops like wheat. With the rising demands worldwide for food security and healthy cultivation, the application of HSI in agro-diagnostics has expanded considerably. This paper provides a comprehensive and state-of-the-art review of hyperspectral imaging strategies devoted to wheat disease discrimination. It essentially introduces the theoretical backgrounds of HSI, such as data acquisition, preprocessing and spectral-spatial feature extraction. The survey further details a plethora of analytical approaches from classical statistical learning methods to deep learning and their utility in modelling HSI data. In particular, a comparative study of these methods is carried out and discussed for distinguishing healthy and diseased wheat, as well as different types of diseases under diverse environmental conditions. The paper also considers the benchmark datasets, sensors and platforms (field/laboratory-based) for which there are practical limitations. Key challenges are addressed, such as data dimensionality, variability as a consequence of atmospheric conditions and the requirement for online implementation in open-field scenarios. A set of suggestions for applying HSI in other domains has been proposed, such as the fusion of HSI with additional remote sensing information, introduction of compact models to edge devices and construction of a scalable and economical solution of HSI in commercial agriculture.

Key words: Deep learning, Hyperspectral imaging, Plant pathology, Precision agriculture, Spectral analysis, Wheat disease detection.

Wheat is the most extensively produced cereal in the world and one of the main direct sources of sustenance for humans. But wheat is always under threat from many diseases such as leaf rust, stem rust, powdery mildew, Septoria blotch and blight. These diseases are important hazards to productivity and grain quality with major financial losses and threats to food security if not adequately controlled (Mahlein, 2016; Terentev *et al.*, 2023).

Traditional disease identification in wheat is primarily based on visual inspection of the field by the human eye. These are fast, on-the-spot analyses, but they are also inherently slow, inefficient and subjective or inconsistent. Furthermore, they are not scalable enough for large-scale agricultural applications, particularly in resource-limited regions (Mahlein, 2016; Wahabzada *et al.*, 2016).

However, hyperspectral imaging (HSI) has been widely regarded as a robust, non-invasive remote sensing technology to monitor delicate plant physiological and biochemical responses (Hilton *et al.*, 2021; Mahlein, 2016; Gogoi *et al.*, 2018). Unlike conventional red-green-blue (RGB) photography that acquires information in just three spectral bands, HSI acquires data in hundreds of closely spaced, adjacent wavelength intervals across the image to enable the extraction of pixel-level spectra (Hilton *et al.*, 2021; Gogoi *et al.*, 2018). The high resolution spectral data permits early and precise diagnosis of plant stress signals, sometimes before they can be seen by the naked eye (Mahlein, 2016; Xie *et al.*, 2017; Terentev *et al.*, 2023).

[1]Department of Computer Science, Presidency University, Bengaluru-560 089, Karnataka, India.
[2]Department of Computer Engineering, Presidency University, Bengaluru-560 064, Karnataka, India.

Corresponding Author: M. Deepak, Department of Computer Science, Presidency University, Bengaluru-560 089, Karnataka, India. Email: deepak.neo.m@gmail.com

How to cite this article: Deepak, M. and Shyam, G.K. (2026). Hyperspectral Imaging for Disease Detection in Wheat Crops: A Comprehensive Survey. *Indian Journal of Agricultural Research*. **60(11):** 1639-1654. doi: 10.18805/IJARe.A-6533.

Submitted: 05-03-2026 **Accepted:** 22-06-2026 **Online:** 02-09-2026

Several reviews on the applications of remote sensing and machine learning for plant disease detection have been conducted, but they have mainly considered broad crop categories or general methodological overviews, rather than specifically focusing on the wheat crop or systematically comparing classical and deep learning paradigms in an HSI framework (Behmann *et al.*, 2015; García-Vera *et al.*, 2024; Kamilaris and Prenafeta-Boldú, 2018; Li *et al.*, 2019; Gogoi *et al.*, 2018; Gupta and Soni, 2022). There is no thorough and focused evaluation in the literature that consolidates HSI-based methodologies, benchmark datasets, sensor platforms and deployment problems for wheat disease detection.

The present review attempts to fill these gaps by targeting the following specific objectives: (i) to present the basic principles of hyperspectral imagery and pre-processing techniques, (ii) to review feature extraction strategies and machine/deep learning-based classification methods for wheat disease detection, (iii) to discuss available datasets and sensor platforms and (iv) to evaluate challenges in practical use and future prospects for scalable HSI deployments in field-scale wheat monitoring. To the best of authors' knowledge, this is the first review that thoroughly integrates the above features especially in the context of HSI-based wheat disease detection.

Review methodology

The review was performed through systematic search of peer-reviewed literature from 2015 to 2025. The main databases consulted were Web of Science, Scopus, IEEE Xplore, Google Scholar and PubMed. The search was conducted using a combination of the following keywords: "hyperspectral imaging", "wheat disease detection", "precision agriculture", "spectral imaging", "deep learning crop disease", "remote sensing wheat", "plant disease classification" and "hyperspectral image classification" (Behmann *et al.*, 2015; García-Vera *et al.*, 2024; Hilton *et al.*, 2021; Kamilaris and Prenafeta-Boldú, 2018; Li *et al.*, 2019; Mahlein, 2016; Rasti *et al.*, 2018).

Studies were included in this review if they (i) used hyperspectral imaging as the main sensing modality, (ii) targeted wheat or other cereal crops that are phylogenetically close for disease detection or classification, (iii) provided quantitative performance metrics such as classification accuracy, F1-score, or overall accuracy and (iv) were published in peer-reviewed journals or reputable conference proceedings (Abdulridha *et al.*, 2023; Chang *et al.*, 2024; Chossegros *et al.*, 2025; Carvalho *et al.*, 2025; Erdilo *et al.*, 2025; Fedotov *et al.*, 2025; Feng *et al.*, 2020; Feng *et al.*, 2022; Goyal *et al.*, 2025; Haagsma *et al.*, 2023; Hilton *et al.*, 2021; Khan *et al.*, 2021; Li *et al.*, 2019; Li *et al.*, 2020; Mahlein, 2016; Mortensen *et al.*, 2020; Rasti *et al.*, 2018; Terentev *et al.*, 2023; Ualiyeva *et al.*, 2025; Wang *et al.*, 2019; Xie *et al.*, 2017; Xu *et al.*, 2018; Zhang *et al.*, 2019; Zhang *et al.*, 2016; Zhong *et al.*, 2022; Gogoi *et al.*, 2018). Studies were excluded if they: (i) were based on RGB or conventional multispectral imaging only and did not include hyperspectral data; (ii) included other crops with no direct methodological implications for HSI-based disease detection; (iii) were conference abstracts, editorials or short communications that did not provide sufficient methodological detail; or (iv) were published before 2015, given the rapid pace of development of deep learning techniques in this area (Kamilaris and Prenafeta-Boldú, 2018; Krizhevsky *et al.*, 2012; Li *et al.*, 2019; Gupta and Soni, 2022).

After the application of these criteria, 36 studies were found and included in the final synthesis [1-36]. The studies were systematically classified and analysed along the following dimensions: (i) HSI acquisition platform (UAV-based, ground-based, or satellite-based); (ii) pre-processing and feature extraction strategies; (iii) classification methodology (classical machine learning vs. deep learning); (iv) wheat disease type investigated and (v) dataset characteristics including spectral range, spatial resolution and availability (Abdulridha *et al.*, 2023; Chossegros *et al.*, 2025; Feng *et al.*, 2020; Feng *et al.*, 2022; Haagsma *et al.*, 2023; Li *et al.*, 2019; Rasti *et al.*, 2018; Zhang *et al.*, 2019; Zhong *et al.*, 2022; Gogoi *et al.*, 2018; Gupta and Soni, 2022). This analytical approach sets the basis for the comparative discussions in later parts.

Fundamentals of hyperspectral imaging

Hyperspectral imaging (HSI) is an advanced technique of remote sensing and it involves the collection of rich spectral information across a broad range of electromagnetic spectrum (Hilton *et al.*, 2021; Mahlein, 2016; Rasti *et al.*, 2018). Contrary to classical imaging systems that collect data in a few distinct bands (red, green and blue RGB), HSI captures hundreds of contiguous and narrow spectral bands for each spatial position within a scene (Hilton *et al.*, 2021; Rasti *et al.*, 2018). This enables distinguishing between minor variations in material composition, structure and physiology associated with their respective specific spectral fingerprints (Mahlein, 2016; Wahabzada *et al.*, 2016).

Hyperspectral image (HSI) The primary product of an HSI system is the hyperspectral datacube, or spectral image cube. This 3D image comprises two spatial dimensions (x, y) and one spectral dimension (λ), where each pixel in the lateral plane has a continuous reflectance spectrum over a defined wavelength region, which are usually found invisible-near infrared or shortwave infrared regions (Hilton *et al.*, 2021; Rasti *et al.*, 2018; Zhang *et al.*, 2019).

This high-spectral information offers accurate measurement of plant properties, including chlorophyll content, water status, pigments concentration and impaired disease physiologic activity-decades before visible symptoms occur (Mahlein, 2016; Wahabzada *et al.*, 2016). In agriculture, especially crop disease detection, HSI has the ability to discriminate between healthy and diseased tissues at an early stage very efficiently used as a diagnostic tool (Feng *et al.*, 2020; Haagsma *et al.*, 2023; Mortensen *et al.*, 2020; Terentev *et al.*, 2023; Xie *et al.*, 2017).

Spectral data cube

The hyperspectral data cube is an object whose organizational or structural concept is a three-dimensional array with two spatial dimensions (usually in reference to corresponding x and y coordinates of an image) and one spectral dimension, defined over hundreds of consecutive wavelength bands (Hilton *et al.*, 2021; Rasti *et al.*, 2018). This setup enables hyperspectral imaging to acquire spatial patterns and full spectral peaks for each pixel of a scene (Hilton *et al.*, 2021; Rasti *et al.*, 2018; Zhang *et al.*, 2019). Unlike conventional imaging methods, which

contain only surface color information, the spectral data contained in the cube can be used to identify subtle biochemical and physiological changes found in plant tissues (Mahlein, 2016; Wahabzada *et al.*, 2016).

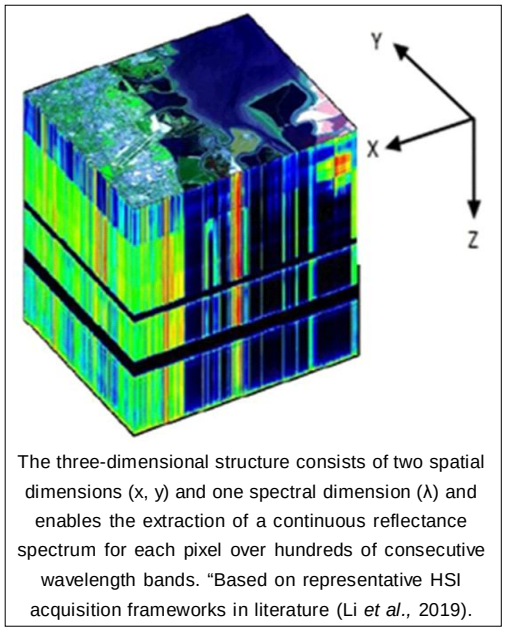
Certain areas of the electromagnetic spectrum are especially useful for plant health diagnosis (Hilton *et al.*, 2021; Mahlein, 2016). The visible (VIS: 400-700 nm) range records pigmentation changes, in particular of chlorophyll and carotenoids (Hilton *et al.*, 2021; Mahlein, 2016). In the visible to the near-infrared (vis-NIR: 400-700 nm) spectral region, the response is related to internal leaf structure and cell integrity, whereas in a longer-range of wavelengths (the shortwave infrared: SWIR 1100-2500 nm), it responds to water content, lignin and other biochemical components (Hilton *et al.*, 2021; Mahlein, 2016; Wahabzada *et al.*, 2016). By measuring reflectance changes in these bands, hyperspectral systems allow stress-related physiological traits to be observed (for example origin of the stress) so that disease resistance can be assessed at anearlier stage than visual assessment (Feng *et al.*, 2020; Haagsma *et al.*, 2023; Mortensen *et al.*, 2020; Terentev *et al.*, 2023; Xie *et al.*, 2017). This specific capacity to combine the spatial and spectral information makes hyperspectral imaging a powerful tool for accurate and early diagnosis of diseases in plants, which are necessary for precision agriculture techniques and sustainable crop management practices (Behmann *et al.*, 2015; Hilton *et al.*, 2021; Mahlein, 2016; Wahabzada *et al.*, 2016).

Imaging modalities

- Pushbroom or line-scan sensors are commonly used for airborne and satellite platforms (Hilton *et al.*, 2021; Mortensen *et al.*, 2020). One spatial-line is recorded at a time by these sensors while the platform advances, thus incrementally composing the hyperspectral data cube (Hilton *et al.*, 2021). This technique has high spectral resolution and is particularly appropriate for applications demanding detailed mapping across large areas (Hilton *et al.*, 2021; Rasti *et al.*, 2018). Pushbroom sensors are effective and compatible with Unmanned Aerial Vehicles (UAVs) and thus have been widely used for the application of agricultural inspection, such as crop disease detection (Abdulridha *et al.*, 2023; Feng *et al.*, 2020; Haagsma *et al.*, 2023; Mortensen *et al.*, 2020; Terentev *et al.*, 2023). The sensor selection has to be done depending on the application scenarios including aerial borne, satellite-based or in a controlled laboratory setting (Hilton *et al.*, 2021; Mahlein, 2016).
- Whiskbroom (or point-scan) sensors move a rotating mirror to scan across the scene on a per-point or per-strip basis (Hilton *et al.*, 2021). Slower at capturing data compared to the pushbroom (whisk is slower than broom!), whiskbroom sensors can have a higher signal-to-noise ratio and are commonly found in satellite imaging (Hilton *et al.*, 2021; Rasti *et al.*, 2018). But their mechanical intricacy has limited their applicability in UAV deployment (Hilton *et al.*, 2021; Mortensen *et al.*, 2020).
- Snapshot (or area-scan) sensors record the complete hyperspectral data cube in a single exposure with no scanning movement (Hilton *et al.*, 2021). Such systems are extremely useful when operating in a dynamically system or real time system environment, *e.g.* laboratory plant phenotyping or robotics system setting (Hilton *et al.*, 2021; Mahlein, 2016; Wahabzada *et al.*, 2016). They are usually limited by lower spatial and spectral resolution as well as restricted to smaller wavelength range because of the sensor or hardware issues (Hilton *et al.*, 2021; Rasti *et al.*, 2018).

For the design of hyperspectral imaging systems for concrete agricultural uses, these imaging modalities must be understood, as each has its consequences on the type of data acquired, processing requirements and deployment potential in field conditions (Fig 1).

HSI systems are generally based on one of three most common EPI acquisition modalities: Pushbroom, whiskbroom, or snapshot mode (Hilton *et al.*, 2021; Rasti *et al.*, 2018). Features of all these sensors, the pushbroom ones particularly, make them useful for agricultural monitoring due to their ability to efficiently collect high-resolution spectral information in aerial campaigns (Hilton *et al.*, 2021; Mortensen *et al.*, 2020). When coupled with UAV platforms, pushbroom systems allow for fast and large area data acquisition of crop fields; thus they are highly effective in perceiving the spatial patterns of plant stress and disease at a high spectral resolution (Abdulridha *et al.*, 2023; Feng *et al.*, 2020; Haagsma *et al.*, 2023; Mortensen *et al.*, 2020; Terentev *et al.*, 2023).



The three-dimensional structure consists of two spatial dimensions (x, y) and one spectral dimension (λ) and enables the extraction of a continuous reflectance spectrum for each pixel over hundreds of consecutive wavelength bands. "Based on representative HSI acquisition frameworks in literature (Li *et al.*, 2019).

Fig 1: Conceptual illustration of a hyperspectral data cube gathered over a wheat field.

Spectral signatures of wheat diseases

Wheat diseases induce a range of physiological and bio chemical changes in the plant, including chlorophyll content, water content, cell structure and pigment constitution alterations. These internal perturbations appear as small but measurable changes in the plant spectral reflectance profile within certain wavebands (Mahlein, 2016; Wahabzada *et al.*, 2016). Hyperspectral imaging (HSI) systems can be utilized to acquire these spectral signatures accurately and provide a means for non-destructive detection, classification and mapping of different wheat diseases in both the latent as well as distinguishable stage(s) of infection (Feng *et al.*, 2020; Haagsma *et al.*, 2023; Mortensen *et al.*, 2020; Terentev *et al.*, 2023; Xie *et al.*, 2017). By examining reflectance anomalies in targeted spectral bands, especially over the visible, near-infrared and shortwave-infrared regions of the spectrum, HSI allows for early warning and improved crop health management strategies (Hilton *et al.*, 2021; Mahlein, 2016; Terentev *et al.*, 2023; Ualiyeva *et al.*, 2025).

Common diseases

a. Leaf rust (*Puccinia triticina*)- Reduction in chlorophyll gives rise to Causes red-orange pustules and hinder in photosynthesis (Terentev *et al.*, 2023; Xie *et al.*, 2017).

b. Stem rust (*P. graminis*)- Affects tissue results in More severe, affects vascular tissues (Abdulridha *et al.*, 2023; Fedotov *et al.*, 2025).

c. Powdery mildew (*B. graminis*)- Ends up as White powder on leaf surfaces (Feng *et al.*, 2022).

d. Septoria blotch (*Z. tritici*)- It results in necrotic lesions and reduced green leaf area (Chossegros *et al.*, 2025).

These changes cause:

- Decreased NIR reflectance (700-1000 nm) (Mahlein, 2016; Wahabzada *et al.*, 2016).
- Increased VIS reflectance (400-700 nm) (Mahlein, 2016; Wahabzada *et al.*, 2016).
- Alterations in SWIR water absorption bands (1450, 1950 nm) (Hilton *et al.*, 2021; Mahlein, 2016).

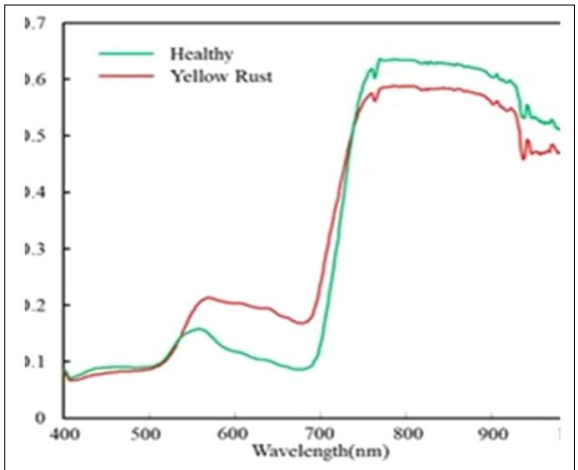
Spectral changes

The first requirement for classifying and analyzing data is to prepare the images through some preprocessing steps that improve the quality of hyperspectral image and facilitate the processing and interpretation. The raw HSI data is generally corrupted by different kinds of noise and artifacts such as sensor noise, non-uniform illumination, atmospheric distortion or redundant spectral information. These difficulties require pre- processing methods (spectral smoothing, radiometric calibration, geometric correction and illumination normalization) to remove the influence of environmental/environmental changes and instrument characteristics (Behmann *et al.*, 2015; Li *et al.*, 2019; Rasti *et al.*, 2018; Zhang *et al.*, 2019).

The wheat diseases trigger specific physiological stress responses which change the leaf pigment content and internal water distribution, that are known to arrest importantly on the plant's spectral reflectance characteristics (Mahlein, 2016; Wahabzada *et al.*, 2016). These changes are more significant in the Visible (VIS: 400-700 nm), Near- IR (NIR: 700-1000 nm) and Short-wavelength IR (SWIR: 1000-2500 nm) spectral ranges relevant for remote sensing for crop health monitoring (Hilton *et al.*, 2021; Mahlein, 2016).

Some of the important spectral variations in the diseased wheat leaves are (Fig 2).

- **Decreased NIR reflectance (700-1000 nm):** Damage to the leaf cause SAR in the host by collapsed spongy mesophyll, broken intercellular air spaces leading to resolution of NIR since healthy tissue reflects strongly thanks to predominantly unbroken cell walls and coupling with internal organ tissue (Mahlein, 2016; Terentev *et al.*, 2023; Wahabzada *et al.*, 2016).
- **Increased VIS reflectance (400-700 nm):** Pathogen-induced degradation of chlorophyll decreases light absorbance in the blue (450 nm) and red (670 nm) spectra, leading to higher reflectance. This coloration response is frequently expressed as yellowing or chlorosis that can be observed with the naked eye in infected leaves (Mahlein, 2016; Terentev *et al.*, 2023; Xie *et al.*, 2017).
- Changes to the strong water absorbance bands around 1450 nm and 1950 nm in SWIR (Hilton *et al.*, 2021; Mahlein, 2016).
- Infection-mediated changes in leaf water content are reflected as distinct shifts in these absorption features. Cut off values for the water absorption depth may be used as an indication of dehydration when reduced, or tissue



Disease infection is characterized by reduced NIR reflectance, increased VIS reflectance and changes in water absorption characteristics around 1450 nm and 1950 nm. From spectral analysis of wheat pathology (Mahlein, 2016).

Fig 2: Spectral reflectance of healthy and diseased wheat leaves over the visible (VIS: 400-700 nm), near-infrared (NIR: 700-1000 nm) and shortwave infrared (SWIR: 1000-2500 nm) areas.

necrosis or water retention resulting from exacerbation of a disorder when increased (Mahlein, 2016; Wahabzada *et al.*, 2016).

- These wavelength-dependent reflectance anomalies can be exploited by HSI sensors to detect and distinguish healthy and diseased plant regions well before visible symptoms appear (Feng *et al.*, 2020; Haagsma *et al.*, 2023; Mortensen *et al.*, 2020; Terentev *et al.*, 2023; Ualiyeva *et al.*, 2025; Xie *et al.*, 2017).

Preprocessing and feature extraction

Moreover, as hyperspectral images are high-dimensional (sometimes with hundreds of spectral bands), many dimensionality reduction methods have been applied to reduce the size of these data while retaining most informative features and avoiding overfitting (Behmann *et al.*, 2015; Li *et al.*, 2019; Rasti *et al.*, 2018). Common methodologies: The Planetary Data System (PDS) has a list of classification algorithms available for planetary image analysis that include dimensionality reduction methods as PCA and components transformation by Minimum Noise Fraction (MNF), band selection based on statistical differences or obtaining features following the separability rule (Behmann *et al.*, 2015; Li *et al.*, 2019; Rasti *et al.*, 2018; Zhang *et al.*, 2019).

The preprocessing part is an important aspect in the HSI pipeline as it directly affects the performance of classification algorithm applied to subsequent classified disease detection on wheat (Behmann *et al.*, 2015; Li *et al.*, 2019; Rasti *et al.*, 2018; Zhang *et al.*, 2019; Zhong *et al.*, 2022).

Radiometric calibration

Radiometric calibration is a mandatory pre-processing step in hyperspectral image analysis, which converts raw sensor digital numbers (DN) to physically relevant reflectance values (Hilton *et al.*, 2021; Li *et al.*, 2019; Rasti *et al.*, 2018). Raw HSI data is inevitably influenced by sensor-specific responses, dark current noise and non-uniform illumination conditions (Hilton *et al.*, 2021; Rasti *et al.*, 2018). If not calibrated, these artifacts cause systematic inaccuracies that impair the reliability of future spectral analysis and disease classification (Behmann *et al.*, 2015; Li *et al.*, 2019; Rasti *et al.*, 2018). In wheat disease diagnosis, precise recovery of reflectance is crucial, since the spectral changes generated by the illness are frequently modest and can easily be disguised by uncorrected sensor errors (Mahlein, 2016; Terentev *et al.*, 2023; Ualiyeva *et al.*, 2025; Xie *et al.*, 2017). The calibration is normally done with a white Spectral on reference panel of known reflectance qualities, acquired under the same illumination circumstances as the target picture (Hilton *et al.*, 2021; Rasti *et al.*, 2018).

$$R(\lambda) = \frac{W(\lambda) - D(\lambda)}{DN(\lambda) - D(\lambda)} \quad ...(1)$$

Where,

$R(\lambda)$ = Calibrated reflectance at wavelength λ.

$DN(\lambda)$= Raw digital number recorded by the sensor.

$D(\lambda)$= Dark current reference acquired with the lens cap on.

$W(\lambda)$= White reference panel measurement.

This normalization removes distortions produced by the light and the non-uniformity of the sensor response so that the final reflectance values are similar across different acquisition sessions, platforms and environmental conditions (Hilton *et al.*, 2021; Li *et al.*, 2019; Rasti *et al.*, 2018).

Dimensionality reduction - Principal component analysis (PCA)

Hyperspectral captures generally have hundreds of spectral bands, of which a large number are highly correlated and contain redundant information (Li *et al.*, 2019; Rasti *et al.*, 2018). This high dimensionality incurs considerable processing hurdles and may cause the Hughes phenomenon where the performance of the classifier decreases with the increasing number of features with respect to the number of training examples (Behmann *et al.*, 2015; Li *et al.*, 2019; Rasti *et al.*, 2018). Principal Component Analysis (PCA) is a linear unsupervised dimensionality reduction method, which solves this problem by projecting the original high-dimensional spectral data onto a lower-dimensional subspace spanned by the directions of highest variance (Behmann *et al.*, 2015; Li *et al.*, 2019; Rasti *et al.*, 2018). PCA is a frequently used preprocessing approach for HSI based wheat disease diagnosis, to retain the most useful spectral components and remove the noise-dominated bands, which reduces the computing cost and improves the downstream classification performance (Behmann *et al.*, 2015; Fedotov *et al.*, 2025; Li *et al.*, 2019; Rasti *et al.*, 2018; Ualiyeva *et al.*, 2025).

$$Y = XW \quad ...(2)$$

Let $X \in R^{n \times d}$ be the original hyperspectral data matrix with n pixels and d spectral bands.

$W \in R^{d \times x}$ be the matrix of k primary eigen vectors obtained from the covariance matrix:

$$\Sigma = \frac{1}{n} X^T X \quad ...(3)$$

and $Y \in R^{n \times k}$ is the dimensionality-reduced representation containing the k components that explain the greatest share of overall spectral variation. The choice of k is usually chosen by the cumulative explained variance criterion, often set at 95-99% (Behmann *et al.*, 2015; Li *et al.*, 2019; Rasti *et al.*, 2018).

Dimensionality reduction - Linear discriminant analysis (LDA)

PCA is an unsupervised method which discovers directions of maximum variance, while LDA is a supervised dimensionality reduction method which looks for projection paths that maximize the separability among a set of pre-defined classes (Behmann *et al.*, 2015; Li *et al.*, 2019;

Rasti *et al.*, 2018). LDA is advantageous over PCA for hyperspectral wheat disease classification that aims to differentiate between healthy tissue and various disease categories (*e.g.*, leaf rust, stem rust and powdery mildew), because it uses the class label information explicitly to guide the projection (Behmann *et al.*, 2015; Li *et al.*, 2019; Rasti *et al.*, 2018). It has been proven that LDA is able to generate more compact and discriminative feature representation, particularly in the case where the number of spectral bands is substantially bigger than the number of training samples, which is usually the case for agricultural HSI datasets (Behmann *et al.*, 2015; Li *et al.*, 2019; Rasti *et al.*, 2018; Zhong *et al.*, 2022).

$$W^* = \arg\max \frac{|W^T S_B W|}{|W^T S_W W|} \quad ...(4)$$

Where,

S_B is the between-class scatter matrix, defined as:

$$S_B = \sum_{c=1}^{C} n_c (\mu_c - \mu)(\mu_c - \mu)^T \quad ...(5)$$

and S_B is the within-class scatter matrix, defined as:

$$S_B = \sum_{c=1}^{C} \sum_{x \in X_c} (x - \mu_c)(x - \mu_c)^T \quad ...(6)$$

μ_c = Mean of class c.

μ = Global mean.

n_c = Number of samples in class c.

X_c = Set of samples belonging to class c.

The ideal projection maximizes the between-class separability and minimizes the within-class scatter simultaneously, which results in a highly discriminative low-dimensional subspace for multi-class wheat disease classification (Behmann *et al.*, 2015; Li *et al.*, 2019; Rasti *et al.*, 2018; Zhong *et al.*, 2022).

Feature extraction-minimum noise fraction (MNF)

The Minimum Noise Fraction (MNF) transform is a two-stage orthogonal transformation developed for hyperspectral data, which separates spectrally relevant signal components from noise-dominated band (Li *et al.*, 2019; Rasti *et al.*, 2018). MNF differs from PCA in that it first estimates and removes the noise covariance structure and then determines the principal components of the underlying signal, rather than ordering components only on the basis of variance (Li *et al.*, 2019; Rasti *et al.*, 2018). This makes MNF especially suited for airborne and UAV based HSI data in agricultural applications where sensor noise, atmospheric scattering and platform induced vibration can dramatically impact spectrum quality (Abdulridha *et al.*, 2023; Feng *et al.*, 2020; Haagsma *et al.*, 2023; Li *et al.*, 2019; Mortensen *et al.*, 2020; Rasti *et al.*, 2018). In wheat disease detection workflows, MNF is usually applied as the initial preprocessing step and after that, only the leading MNF components, which have the highest signal-to-noise ratio, are kept for further classification (Fedotov *et al.*, 2025; Li *et al.*, 2019; Rasti *et al.*, 2018; Ualiyeva *et al.*, 2025).

$$MNF = \frac{\Sigma_{singal}\, x}{\Sigma_{noise}\, x} \quad ...(7)$$

$\Sigma_{singal}\, x$ = Covariance matrix of the underlying spectral noise.

$\Sigma_{noise}\, x$ = Calculated noise covariance matrix.

The MNF transform consists of two successive PCA steps: The first PCA decorrelates the noise components and normalizes the noise to unit variance; the second PCA is performed on the noise-normalized data (Li *et al.*, 2019; Rasti *et al.*, 2018). The MNF discards the components with eigenvalues near to one as being dominated by noise. The components with much greater eigenvalues include useful spectral information for discriminating between diseases (Behmann *et al.*, 2015; Li *et al.*, 2019; Rasti *et al.*, 2018).

Vegetation index - normalized difference vegetation index (NDVI)

One of the most commonly used spectral indices in remote sensing to evaluate vegetation vigour and detect plant stress is the Normalized Difference Vegetation Index (NDVI) (Hilton *et al.*, 2021; Mahlein, 2016). NDVI utilizes the high contrast between the high reflectance of healthy vegetation in the near-infrared region (due to the interior structure of the leaf cells) and the strong absorption in the red area (due to photosynthesis powered by chlorophyll) (Hilton *et al.*, 2021; Mahlein, 2016; Wahabzada *et al.*, 2016). In sick wheat, pathogen-induced chlorophyll degradation reduces the absorption of red light, while damaging cellular integrity and reducing NIR reflectance, hence causing a detectable reduction in NDVI values (Mahlein, 2016; Terentev *et al.*, 2023; Xie *et al.*, 2017). This renders NDVI a sensitive and computationally effective early indication of disease-induced stress, notably for leaf rust, Septoria blotch and powdery mildew where chlorophyll loss is a key physiological consequence (Chossegros *et al.*, 2025; Feng *et al.*, 2022; Mahlein, 2016; Terentev *et al.*, 2023; Xie *et al.*, 2017).

$$NDVI = \frac{R_{NIR} - R_{red}}{R_{NIR} + R_{Red}} \quad ...(8)$$

Where,

R_{NIR} and R_{red}= Reflectance values at near-infrared (about 800 nm) and red (around 670 nm) wavelengths, respectively.

NDVI values vary from -1 to +1 where values around +1 indicate dense healthy vegetation and decreasing values imply increasing degrees of stress or disease severity (Hilton *et al.*, 2021; Mahlein, 2016). In hyperspectral data sets, NDVI is more accurately derived than in multispectral systems due to the presence of narrowly defined bands at ideal wavelengths (Hilton *et al.*, 2021; Rasti *et al.*, 2018).

Vegetation index - Photochemical reflectance index (PRI)

The photochemical reflectance index (PRI) is a narrow-band spectral index developed to follow dynamic changes in carotenoid pigment composition, specifically the

xanthophyll cycle, which is directly related to photosynthetic light-use efficiency (Hilton *et al.*, 2021; Mahlein, 2016; Wahabzada *et al.*, 2016). The PRI is extremely responsive to early-stage physiological stress prior to the development of observable symptoms, suggesting that the PRI is a useful early warning indication in HSI-based wheat disease monitoring (Feng *et al.*, 2020; Haagsma *et al.*, 2023; Mahlein, 2016; Mortensen *et al.*, 2020; Terentev *et al.*, 2023). As the ratio of carotenoids to chlorophyll changes rapidly with pathogen infection, PRI can identify disease-induced metabolic disruption before any structural damage to the leaf is visible, therefore providing a diagnostic advantage over morphologically based indices such as NDVI (Mahlein, 2016; Wahabzada *et al.*, 2016).

$$PRI = \frac{R_{531} - R_{570}}{R_{531} + R_{570}} \quad ...(9)$$

Where,

R_{531} and R_{570}= Reflectance at 531 nm and 570 nm, respectively.

Reduction of PRI values from healthy baseline measurements are indicative of compromised photosynthetic efficiency and carotenoid pool alterations associated with early illness stress (Mahlein, 2016; Wahabzada *et al.*, 2016). PRI has been shown sensitive to stripe rust and powdery mildew infection in wheat at latent stages, a few days before apparent chlorotic or necrotic signs developed (Feng *et al.*, 2022; Feng *et al.*, 2020; Xie *et al.*, 2017).

Vegetation index - Soil-adjusted vegetation index (SAVI)

The soil-adjusted vegetation index (SAVI) is a variation of NDVI that tries to reduce the influence of soil background light reflectance in the spectral assessment of vegetation (Hilton *et al.*, 2021; Mahlein, 2016). Bare soil reflectance in wheat fields, particularly during the early growth stages when canopy cover is incomplete, can dramatically distort spectral indices and impair the accuracy of disease classification models (Hilton *et al.*, 2021; Mahlein, 2016; Mortensen *et al.*, 2020). However, SAVI overcomes this problem by introducing a soil brightness adjustment factor, which compensates for the differences in soil reflectance under sparse canopy situation, thereby making it more robust than NDVI for disease detection in partially formed or heterogeneous wheat fields (Hilton *et al.*, 2021; Mahlein, 2016; Mortensen *et al.*, 2020).

$$SAVI = \frac{R_{NIR} - R_{Red}(1 + L)}{R_{531} + R_{570} + L} \quad ...(10)$$

Where,

R_{NIR} and R_{Red}= Reflectance values in the near-infrared and red spectral bands respectively.

L is the soil brightness correction factor which is empirically calibrated to 0.5 for moderate vegetation densities (Hilton *et al.*, 2021; Mahlein, 2016). When L=0, SAVI becomes NDVI and for larger values of L the contribution of soil background is more and more suppressed (Hilton *et al.*, 2021; Mahlein, 2016). SAVI is particularly useful in semi-arid wheat producing regions and early season monitoring, where soil exposure is high and traditional NDVI estimations often overestimate vegetation stress (Hilton *et al.*, 2021; Mahlein, 2016; Mortensen *et al.*, 2020).

Vegetation index - Disease water stress index (DSWI)

The disease water stress index (DSWI) is a multi-band spectral index developed to characterize simultaneous changes of the leaf water content and chlorophyll concentration, both affected by the pathogen infection in wheat (Mahlein, 2016; Terentev *et al.*, 2023; Wahabzada *et al.*, 2016). Unlike single-parameter indices, DSWI combines reflectance information from four different wavelength regions that are simultaneously sensitive to water absorption, chlorophyll activity and cell structure integrity, thereby providing a more comprehensive characterization of disease-induced physiological stress (Hilton *et al.*, 2021; Mahlein, 2016; Wahabzada *et al.*, 2016). The DSWI is especially useful in separating disease-related stress from abiotic stressors such as drought, as the spectral band combination uniquely captures pathogen-related tissue degradation patterns that differ from water-deficit responses (Mahlein, 2016; Mortensen *et al.*, 2020; Terentev *et al.*, 2023; Wahabzada *et al.*, 2016).

$$DSWI = \frac{R_{802} - R_{547}}{R_{1657} + R_{682}} \quad ...(11)$$

Where,

R_{802}, R_{547}, R_{1657} and R_{682}= Reflectance values at 802 nm, 547 nm, 1657 nm and 682 nm respectively.

The numerator includes NIR reflectance related to the integrity of leaf cell structure and green reflectance related to carotenoid activity and the denominator includes SWIR water absorption and red chlorophyll absorption properties (Hilton *et al.*, 2021; Mahlein, 2016; Wahabzada *et al.*, 2016). Lower DSWI scores are indicative of concurrent stress on water and chlorophyll, a specific spectral signature of active fungal infection in wheat leaves (Feng *et al.*, 2022; Feng *et al.*, 2020; Haagsma *et al.*, 2023; Mortensen *et al.*, 2020; Terentev *et al.*, 2023; Ualiyeva *et al.*, 2025).

Machine learning and deep learning approaches

Classical classifiers, such as support vector machines (SVM), Random forests (RF) and k-Nearest Neighbors (k- NN), are extensively used in his work have been adopted for hyperspectral image classification due to their robustness and handling of high dimensional data, which need of hand-crafted feature extraction process and domain specific preprocessing steps (Behmann *et al.*, 2015; Li *et al.*, 2019; Rasti *et al.*, 2018). Although such methods have proven useful to some extent for certain cases, they often face challenges in dealing with the intrinsic high-dimensional, spectral redundancy and spatial variation properties of HS image (Behmann *et al.*, 2015; Li *et al.*, 2019; Rasti *et al.*, 2018; Zhang *et al.*, 2019).

However, deep learning methods and especially Convolutional Neural Networks (CNNs), Recurrent Neural Networks (RNNs) and Transformer-based architectures have demonstrated superior classification accuracy and scalability in recent years (Kamilaris and Prenafeta-Boldú, 2018; Krizhevsky *et al.*, 2012; Li *et al.*, 2019; Xu *et al.*, 2018; Zhong *et al.*, 2022). Such models can learn hierarchical spectral-spatial features from raw hyperspectral data automatically and thereby eliminate manually engineered features (Guo *et al.*, 2019; Hang *et al.*, 2019; Li *et al.*, 2019; Li *et al.*, 2020; Wang *et al.*, 2019; Xu *et al.*, 2018; Zhang *et al.*, 2016; Zhong *et al.*, 2022). Besides, deep learning models are more efficient for the generalization of different field conditions, sensor noises and complicated disease shapes could be better adapted to large-scale agricultural monitoring frameworks and real time decision support systems (Chang *et al.*, 2024; Erdilo *et al.*, 2025; Fedotov *et al.*, 2025; García-Vera *et al.*, 2024; Goyal *et al.*, 2025; Khan *et al.*, 2021; Li *et al.*, 2019).

Classical models

Among the classical machine learning methods, SVM, RF, k-NN and DT have been widely applied to analyze hyper-spectral imagery classification tasks (especially in agriculture areas such as disease detection for wheat crops) (Behmann *et al.*, 2015; Li *et al.*, 2019; Rasti *et al.*, 2018). The interpretations and the computational demands are lower with these approaches, which yield competitive performance for small to medium sized datasets (Behmann *et al.*, 2015; Li *et al.*, 2019). However, most of these models rely on manual feature extraction.

Feature extraction

This is also known as point cloud sub-sampling a process of choosing or synthesizing appropriate spectral or spatial features from raw HSIs based on domain knowledge (Behmann *et al.*, 2015; Li *et al.*, 2019; Rasti *et al.*, 2018). Also, the curse of dimensionality is critical problem since hyperspectral images have hundreds of spectral bands, most of which are correlated and noisy (Behmann *et al.*, 2015; Li *et al.*, 2019; Rasti *et al.*, 2018). Consequently, These algorithms are usually optimal only when reducing the dimensionality of data, since using either PCA, LDA considered the version feature selection approaches will reduce the complexity of the feature-space and improve class discrimination (Behmann *et al.*, 2015; Li *et al.*, 2019; Rasti *et al.*, 2018; Zhong *et al.*, 2022).

Despite these limitations, conventional machine learning models are still applicable when the labeled datasets are insufficient or interpretability and model explain ability matter (Behmann *et al.*, 2015; García-Vera *et al.*, 2024; Li *et al.*, 2019).

The discriminant function of a linear SVM is:

$$\text{SVM Decision Funtion: } f(x) = w^{[T]} X + b$$

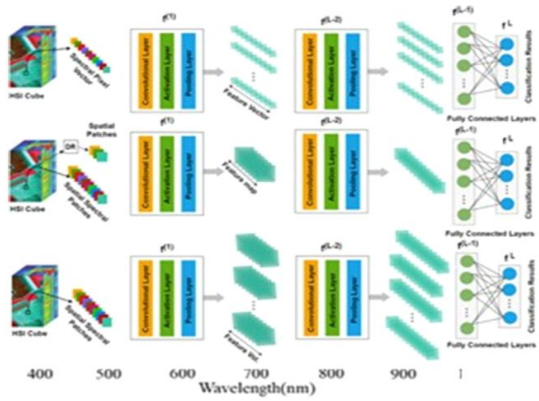
B. Deep learning models

The advent of deep learning models including, among others, Convolutional Neural Networks (CNNs), Recurrent Neural Network (RNNs) and Transformer-based models has greatly boosted hyperspectral image classification by enabling feature hierarchies to be automatically learned from raw input data (Kamilaris and Prenafeta-Boldú, 2018; Krizhevsky *et al.*, 2012; Li *et al.*, 2019; Xu *et al.*, 2018; Zhong *et al.*, 2022). These methods alleviate the heavy dependence of manual feature engineering, since these end-to-end approaches harness large training datasets to learn discriminative spectral-spatial features (Guo *et al.*, 2019; Li *et al.*, 2019; Li *et al.*, 2020; Wang *et al.*, 2019; Xu *et al.*, 2018; Zhang *et al.*, 2016; Zhong *et al.*, 2022; Metagar and Walikar, 2024).

3D Convolutional Neural Networks (3D-CNNs) have shown remarkable performance in hyperspectral image analysis due to their capability of capturing both spectral and spatial information when extracting the features (Li *et al.*, 2019; Xu *et al.*, 2018; Zhong *et al.*, 2022) (Fig 3).

3D-CNNs, by utilization of convolutional filters along the three dimensions of the hyperspectral cube, capture local spectral signature and spatial context simultaneously and can achieve significantly better classification accuracy in particular for fine-grained disease discrimination in crops like wheat (Fedotov *et al.*, 2025; Guo *et al.*, 2019; Khan *et al.*, 2021; Li *et al.*, 2019; Xu *et al.*, 2018; Zhong *et al.*, 2022; Metagar and Walikar, 2024).

Furthermore, RNNs and its variants such as Long-short term memory (LSTM) networks have also been employed on hyperspectral data by considering spectral bands as sequence input, which allows to learn the context relationship between wavelength (Li *et al.*, 2019; Li *et al.*, 2020; Zhong *et al.*, 2022). The latter are particularly useful, when spectral signatures has inherent order due to physiological differences in plant health (Li *et al.*, 2019; Li *et al.*, 2020).



The model is based on three-dimensional convolutional filters that span the spatial and spectral dimensions of the input cube, which allows for the joint learning of the local spectral signatures and the spatial context to enhance the accuracy of wheat disease classification (Zhong *et al.*, 2022).

Fig 3: Architecture of a 3D convolutional neural network (3D-CNN) for joint spectral-spatial feature extraction from hyperspectral image cubes.

In recent years, Vision Transformers (ViTs) and attention has been applied to hyperspectral classification. ViTs being taught to model global relationships over the spectral-spatial domain are capable of providing better context-awareness and feature discrimination (Li *et al.*, 2019; Zhong *et al.*, 2022). Attention mechanisms allow the model to focus selectively to those parts of input instances that are more informative, which is useful, in general, for complex problems such as a disease having subtle or uneven spread of features (Li *et al.*, 2019; Zhong *et al.*, 2022).

Together, these deep learning models present the most advanced hyper-spectral image classification results with improved accuracy, robustness and scalability compared to traditional ML algorithms.

Applications and case studies

There are several cases of real-world hyperspectral imaging (HSI) applications in wheat disease detection that include different systems and scales, which are designed to address the underpinning agricultural monitoring requirements (Abdulridha *et al.*, 2023; Chossegros *et al.*, 2025; Feng *et al.*, 2020; Haagsma *et al.*, 2023; Mortensen *et al.*, 2020; Terentev *et al.*, 2023). These platforms vary on spatial resolution, spectral accuracy, flexibility in operations and cost of deployment (Hilton *et al.*, 2021; Mahlein, 2016).

- **UAV-mounted systems:** Unmanned Aerial Vehicles (UAVs) carrying push broom or snapshot hyperspectral imaging sensors are increasingly used for field scale disease monitoring (Abdulridha *et al.*, 2023; Feng *et al.*, 2020; Haagsma *et al.*, 2023; Mortensen *et al.*, 2020; Terentev *et al.*, 2023). These systems collect multispectral-spatial data at high resolution over specific areas of interest for early disease detection and site-specific application of agrochemicals (Abdulridha *et al.*, 2023; Feng *et al.*, 2020; Mortensen *et al.*, 2020). The UAV-based HSI method is particularly useful for surfacing disease hotspots and guiding site-specific chemical spraying by pesticides or a localized irrigation (Abdulridha *et al.*, 2023; Feng *et al.*, 2020; Mortensen *et al.*, 2020; Terentev *et al.*, 2023) (Fig 4).
- **Ground-based phenotyping platforms:** Operated by tractors or stationery rigs, such platforms are generally utilized in a non-field validated experimental and research environment (Chossegros *et al.*, 2025; Haagsma *et al.*, 2023; Mahlein, 2016; Wahabzada *et al.*, 2016). Provide high-fidelity, short-range hyper-spectral measurements and thus are well suited for examining subtle dynamic shifts in physiology accompanying disease evolution (Chossegros *et al.*, 2025; Haagsma *et al.*, 2023; Mahlein, 2016; Wahabzada *et al.*, 2016). Such systems are essential in validating remote sensing algorithms and for the development of wheat varieties with resistance to disease (Chossegros *et al.*, 2025; Haagsma *et al.*, 2023; Mahlein, 2016).
- **Satellite-based hyperspectral sensors:** Hyperspectral satellite missions (*e.g.,* PRISMA, EnMAP) are at the moment spectrally limited with respect to UAV- and ground-based instruments, but they could potentially revolutionize large-scale agricultural monitoring (Hilton *et al.*, 2021; Rasti *et al.*, 2018). Such systems are useful for regional or national surveillance operations and allow the monitoring of disease events across large-scale geographical areas but at a cost in time frequency of detection (and loss of sensor quality) (Hilton *et al.*, 2021; Mahlein, 2016; Rasti *et al.*, 2018).

In recent times, it has been demonstrated that the joint use of hyperspectral imaging and deep learning models like 3D Convolutional Neural Networks (3D-CNNs) or Vision Transformer models contribute to an early diagnosis of wheat diseases (Audebert *et al.*, 2018; Chang *et al.*, 2024; Chossegros *et al.*, 2025; Erdilo *et al.*, 2025; Fedotov *et al.*, 2025; Khan *et al.*, 2021; Li *et al.*, 2019; Ualiyeva *et al.*, 2025; Zhong *et al.*, 2022). In a number of studies, such methods have reached diagnostic accuracy rates above 90 per cent even when symptoms were not yet evident by eye (Chang *et al.*, 2024; Chossegros *et al.*, 2025; Erdilo *et al.*, 2025; Fedotov *et al.*, 2025; Khan *et al.*, 2021;

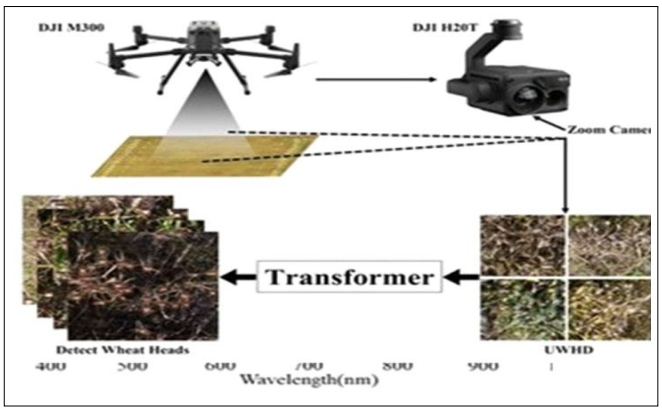


Fig 4: UAV-based wheat-head image acquisition and transformer-based detection workflow, illustrating the use of a DJI Matrice M300 RTK equipped with a Zenmuse H20T sensor, generation of the UAV Wheat Head Dataset (UWHD) and Transformer-based wheat-head detection. Adapted from Zhu *et al.* (2022).

Li *et al.*, 2019; Ualiyeva *et al.*, 2025; Zhong *et al.*, 2022). This highlights the revolutionary capability of HSI as a digital-agriculture-based sustainable crop protection tool (García-Vera *et al.*, 2024; Hilton *et al.*, 2021; Mahlein, 2016).

Comparison tables

The following tables summarizes the important aspects of hyperspectral imaging technique for wheat disease detection. Table 1 lists key wheat diseases, associated pathogens, the most informative spectral bands and their spectral effects. Table 2 compares commonly used classification models in terms of input type, accuracy and implementation characteristics across classical and deep learning methods.

A comparative summary of representative hyperspectral imaging and machine-learning approaches for wheat disease detection, covering the diseases investigated, sensing platforms, spectral ranges, modelling methods, reported performance, dataset characteristics and key limitations, is presented in Table 3.

Table 1: Wheat diseases, associated pathogens, informative spectral bands and spectral effects.

Disease	Pathogen	Key spectral bands (nm)	Spectral effect
Leaf rust	*Puccinia triticina* (Terentev *et al.*, 2023; Xie *et al.*, 2017)	680-750	Decreased chlorophyll absorption; increased VIS reflectance
Stem rust	*Puccinia graminis* (Abdulridha *et al.*, 2023; Fedotov *et al.*, 2025)	700-900	Reduced NIR reflectance due to vascular tissue damage
Powdery mildew	*Blumeria graminis* (Feng *et al.*, 2022)	450-680	Increased VIS reflectance due to white fungal coating
Septoria blotch	*Zymoseptoria tritici* (Chossegros *et al.*, 2025)	600-800	Decreased VIS and NIR reflectance due to necrotic lesions
Fusarium head blight	*Fusarium graminearum* (Erdilo *et al.*, 2025)	550-750	Altered pigment and water content in grain tissue

Table 2: Comparison of classification models for hyperspectral image-based wheat disease detection.

Model	Type	Input	Spectral range (nm)	Reported Accuracy	Dataset/ Platform	Key characteristics
SVM (Behmann *et al.*, 2015; Terentev *et al.*, 2023; Xie *et al.*, 2017)	Classical ML	Spectral vectors	400-1000	85-92%	Field/UAV	Fast training; requires manual feature extraction; effective for small datasets
Random forest (Abdulridha *et al.*, 2023; Feng *et al.*, 2022)	Classical ML	Spectral vectors	400-1000	80-90%	Field/Ground	Robust to noise; handles high-dimensional data; interpretable
k-NN (Behmann *et al.*, 2015; Rasti *et al.*, 2018)	Classical ML	Spectral vectors	400-2500	78-88%	Laboratory	Simple; sensitive to dimensionality; computationally expensive at inference
2D CNN (Khan *et al.*, 2021; Li *et al.*, 2019)	Deep learning	Spatial patches	400-1000	88-94%	UAV/Ground	Captures spatial features; does not exploit spectral correlations fully
3D CNN (Li *et al.*, 2019; Xu *et al.*, 2018; Zhong *et al.*, 2022)	Deep learning	Spectral-spatial cube	400-2500	90-97%	UAV/Laboratory	Simultaneous spectral-spatial feature learning; computationally intensive
Vision transformer ViT (Chang *et al.*, 2024; Zhong *et al.*, 2022)	Deep learning	Spectral-spatial cube	400-2500	93-98%	Laboratory/UAV	Global context modelling; requires large labelled datasets
LSTM/RNN (Li *et al.*, 2019; Li *et al.*, 2020)	Deep learning	Spectral sequences	400-1000	87-93%	Laboratory	Models sequential spectral relationships; useful for temporal disease progression

Major shortcomings of existing hsi systems

Spectral-spatial resolution trade-off

This inverse link between spectral resolution, spatial resolution and acquisition speed is a fundamental engineering limitation in HSI system design (Hilton *et al.*, 2021; Mahlein, 2016; Rasti *et al.*, 2018). Pushbroom sensors on UAV platforms have excellent spectral resolution but are limited in the ability to sustain high spatial resolution over broad field regions concurrently (Abdulridha *et al.*, 2023; Feng *et al.*, 2020; Haagsma *et al.*, 2023; Mortensen *et al.*, 2020; Rasti *et al.*, 2018). Snapshot sensors increase acquisition speed, albeit at the cost of spectral and spatial resolution (Hilton *et al.*, 2021; Rasti *et al.*, 2018). None of the commercial HSI platforms available on the market today fully solve this three-way trade-off and the best sensor combination is still application-specific and depends on the disease type, the stage of crop growth and the field scale (Hilton *et al.*, 2021; Mahlein, 2016; Rasti *et al.*, 2018).

Calibration instability under field conditions

Compared to controlled laboratory settings, radiometric calibration is far more difficult in the dynamic field environment due to fluctuations in sun irradiation, solar zenith angle and crop movement generated by wind during acquisition (Hilton *et al.*, 2021; Li *et al.*, 2019; Rasti *et al.*, 2018). The majority of the studies that were evaluated execute the calibration using a single white reference panel acquired at the beginning of the flight mission and do not account for the change in illumination during the data collection (Abdulridha *et al.*, 2023; Feng *et al.*, 2020; Haagsma *et al.*, 2023; Mortensen *et al.*, 2020). This calibration instability causes systematic spectral errors that could lower classification accuracy by 3-8 percentage points in realistic field situations relative to laboratory benchmarks (Haagsma *et al.*, 2023; Mahlein, 2016; Rasti *et al.*, 2018). Although the performance of the model is significantly affected by calibration uncertainty, it is rarely quantified or explicitly mentioned in the reviewed literature (Hilton *et al.*, 2021; Li *et al.*, 2019; Rasti *et al.*, 2018).

Lack of standardised benchmark datasets

The present HSI wheat disease research is critically limited by the lack of large-scale, publicly available and standardized benchmark datasets that would allow for a credible cross-study comparison (Behmann *et al.*, 2015; García-Vera *et al.*, 2024; Kamilaris and Prenafeta-Boldú, 2018; Li *et al.*, 2019). Most of the evaluated research create their own datasets for specific local conditions, wheat varieties, disease strains and growth phases (Abdulridha *et al.*, 2023; Chossegros *et al.*, 2025; Fedotov *et al.*, 2025; Feng *et al.*, 2020; Feng *et al.*, 2022; Goyal *et al.*, 2025; Haagsma *et al.*, 2023; Khan *et al.*, 2021; Mortensen *et al.*, 2020; Terentev *et al.*, 2023; Ualiyeva *et al.*, 2025). The dataset sizes range from less than 500 to several thousand tagged samples (Abdulridha *et al.*, 2023; Chossegros *et al.*, 2025; Fedotov *et al.*, 2025; Khan *et al.*, 2021; Mortensen *et al.*, 2020; Terentev *et al.*, 2023). This lack of diversity greatly limits the generalisability of trained models and makes it impossible to know if accuracy improvements claimed are due to actual methodological progress or benign dataset factors (Kamilaris and Prenafeta-Boldú, 2018; Li *et al.*, 2019; Zhong *et al.*, 2022). Perhaps the most important contribution that might be made to speed real progress in this sector is the construction of a community-standard HSI wheat disease benchmark dataset (Behmann *et al.*, 2015; Kamilaris and Prenafeta-Boldú, 2018; Li *et al.*, 2019).

Computational infrastructure requirements

The computational needs of deep learning-based hyperspectral image (HSI) processing pipelines are a major practical challenge for field deployment, since the processing of a single UAV flight mission producing several terabytes of hyperspectral data calls for large GPU computing resources (Li *et al.*, 2019; Xu *et al.*, 2018; Zhong *et al.*, 2022). Such processing delays are fundamentally at odds with the real-time or near-real-time decision support needs of operational agriculture (García-Vera *et al.*, 2024; Li *et al.*, 2019; Mahlein, 2016). Although considerable research on lightweight model architectures and edge computing solutions is underway, there is no commercial HSI-based wheat disease detection system available today at the speed, cost and reliability necessary for routine adoption at the farm scale (Chang *et al.*, 2024; Li *et al.*, 2019; Xu *et al.*, 2018; Zhong *et al.*, 2022). This gap between research-grade system performance and commercial deployment readiness remains a major open challenge in the area (Kamilaris and Prenafeta-Boldú, 2018; Li *et al.*, 2019; Zhong *et al.*, 2022).

A rigorous comparison of deep learning models

2D CNN vs. 3D CNN

While 2D CNNs are computationally efficient, they cannot explicitly describe the sequential spectral correlations between consecutive wavelength bands. 3D-CNNs employ convolutional filters over both spatial and spectral dimensions simultaneously (Li *et al.*, 2019; Xu *et al.*, 2018; Zhong *et al.*, 2022). The evaluated papers consistently report that 3D-CNNs outperform 2D-CNNs by 3-6 percentage points in terms of overall accuracy, but at a computational cost of around 4-8 times more parameters, rendering them not suitable for edge deployment (Fedotov *et al.*, 2025; Khan *et al.*, 2021; Li *et al.*, 2019; Xu *et al.*, 2018; Zhong *et al.*, 2022).

CNN or vision transformer (ViT)

CNNs are good at modeling the local spectral-spatial linkages through hierarchical convolution (Li *et al.*, 2019; Xu *et al.*, 2018; Zhong *et al.*, 2022). Vision Transformers explore the long-range global dependencies over the full spectral-spatial domain using self-attention processes at the same time (Chang *et al.*, 2024; Li *et al.*, 2019; Zhong *et al.*, 2022). ViT-based architectures produce the greatest

Table 3: Comprehensive comparison of recent studies on HSI-based wheat disease detection.

Reference	Year	Disease	Sensor/Platform	Spectral Range (nm)	Method	Accuracy (%)	Dataset size	Limitations
Xie *et al.*	2017	Stripe rust	Pushbroom/UAV	400-1000	SVM + PCA	88.4	Field-scale	Limited to single disease; no deep learning
Feng *et al.*	2020	Stripe rust	UAV-mounted HSI	400-1000	RF + NDVI	91.2	UAV field plots	No spectral-spatial joint modelling
Mortensen *et al.*	2020	Multiple diseases	UAV/Thermal fusion	400-2500	CNN	90.5	Controlled field	Small dataset; limited generalisability
Khan *et al.*	2021	Leaf Rust, Powdery Mildew	Ground-based HSI	400-2500	Deep CNN	94.3	Laboratory	Lab conditions only; not field-validated
Abdulridha *et al.*	2023	Stem rust	Drone HSI	400-1000	SVM, RF	89.7	Drone field plots	Limited spatial resolution
Terentev *et al.*	2023	Leaf rust	Ground/UAV HSI	450-950	ML ensemble	92.1	Multi-location field	High sensor cost; weather dependency
Haagsma *et al.*	2023	Soil-borne mosaic Virus	Ground/Field HSI	400-2500	SVM + band selection	87.5	Lab to field	Lab-to-field transferability issues
Feng *et al.*	2022	Powdery mildew	Ground-based HSI	350-2500	SVM, RF, ANN	93.6	Controlled greenhouse	Greenhouse only; no UAV deployment
Chang *et al.*	2024	Leaf/Stem rust	Field RGB+HSI	400-700	DenseNet (improved)	95.2	Large field dataset	RGB-dominant; limited SWIR bands
Ualiyeva *et al.*	2025	Multiple diseases	VNIR HSI/Ground	400-1000	ML classifiers	91.8	Multi-variety field	VNIR only; no SWIR integration
Chossegros *et al.*	2025	Multiple infections	Lab HSI	400-2500	CNN-based	96.4	Controlled lab	Lab setting; not field-deployable yet
Fedotov *et al.*	2025	Stem rust	UAV/Ground HSI	400-1000	Advanced ML + HSI	93.9	Multi-site field	Computational cost; data volume
Erdilo *et al.*	2025	Fusarium head blight	UAV HSI	400-1000	Deep learning	95.7	Field plots	Limited disease classes
Goyal *et al.*	2025	Leaf disease (intercrop)	Ground HSI	400-2500	Hybrid deep learning	97.1	Multi-crop field	Multi-crop setting; wheat-specific validation needed

reported accuracies of 93-98%, exceeding 3D-CNNs by 2-4 percentage points, but require considerably larger labelled training datasets and may perform worse on the short agricultural HSI datasets that are typical of most wheat disease investigations (Chang *et al.*, 2024; Li *et al.*, 2019; Zhong *et al.*, 2022).

RNN and LSTM in spectral sequence modeling

RNNs and LSTMs model hyperspectral data as ordered spectral sequences and utilize the continuity of reflectance across neighbouring wavelength bands to capture slow spectral changes associated with disease development (Li *et al.*, 2019; Li *et al.*, 2020; Zhong *et al.*, 2022). However, their incapability to include spatial context restricts the performance 20, 21. Hybrid designs of LSTM spectral modelling and CNN spatial feature extraction have shown a more practical accuracy range of 90-95% (Khan *et al.*, 2021; Li *et al.*, 2019; Li *et al.*, 2020; Xu *et al.*, 2018).

Hybrid and ensemble architectures

The latest hybrid architectures that merge CNN spatial feature extraction with Transformer based global spectrum attention have achieved the highest reported accuracies, but at a considerable expense of architectural complexity, training data needs and inference time (Chang *et al.*, 2024; Goyal *et al.*, 2025; Li *et al.*, 2019; Zhong *et al.*, 2022). Ensemble approaches integrating many independently trained classifiers provide a pragmatic alternative with competitive accuracy and less need on huge labelled datasets making them well suited for real world agricultural deployment (Abdulridha *et al.*, 2023; Feng *et al.*, 2022; Terentev *et al.*, 2023).

Practical use for farmers and commercialization

Economic availability

The cost of commercial UAV-mounted HSI sensors ranges from USD 20,000 to USD 80,000, which is prohibitive for most wheat producers globally, especially smallholder farmers in underdeveloped nations (Hilton *et al.*, 2021; Mahlein, 2016; Rasti *et al.*, 2018). Technology development or service-based deployment methods for farmers to receive disease detection via agricultural cooperatives or precision agriculture providers will be necessary to greatly reduce hardware costs and achieve commercial viability (García-Vera *et al.*, 2024; Mahlein, 2016).

Ease of use and operation by farmers

In addition to cost issues, effective HSI data collecting needs technical skills in flight planning, sensor calibration and data quality control that cannot be assumed of normal farm operators (Haagsma *et al.*, 2023; Khan *et al.*, 2021; Mahlein, 2016). Widespread adoption of end to end HSI systems requires automated calibration and one-click processing pipelines, with simple map-based outputs that can be directly used in spray prescription or harvesting decision making workflows without the need for specialist expertise (García-Vera *et al.*, 2024; Khan *et al.*, 2021; Li *et al.*, 2019).

Integration of decision support

The practical significance of disease detection using HSI is not only in classification accuracy, but also in how the results are transformed into economically effective and timely management decisions, coupled to yield loss models, treatment cost thresholds and weather forecast data (Hilton *et al.*, 2021; Li *et al.*, 2019; Rasti *et al.*, 2018). Without this decision support integration layer, even very accurate disease maps have limited operational utility for farmers who need to turn spectral data into specific field management activities under real-world constraints (García-Vera *et al.*, 2024; Li *et al.*, 2019; Mahlein, 2016).

Validation and regulatory requirements

Before HSI-based disease detection systems can be used commercially, independent validation across a range of geographic regions, wheat varieties, disease strains and seasons is required, a requirement that has not been comprehensively addressed in the literature to date (Behmann *et al.*, 2015; García-Vera *et al.*, 2024; Kamilaris and Prenafeta-Boldú, 2018; Li *et al.*, 2019). The current research landscape is mainly absent this regulatory dimension which is a crucial precondition for responsible commercial implementation, defined by internationally accepted validation processes and minimum performance criteria (García-Vera *et al.*, 2024; Kamilaris and Prenafeta-Boldú, 2018; Li *et al.*, 2019).

Scalability with data as a service models

A viable route to economic feasibility is through federated, data-as-a-service models where HSI disease detection is provided by satellite or aerial survey services combined with cloud-based AI processing platforms, removing the need for farm-level hardware investment (García-Vera *et al.*, 2024; Hilton *et al.*, 2021; Mahlein, 2016). Satellite-based HSI platforms, such as PRISMA and EnMAP, together with automated deep learning pipelines, can provide cost-effective regional disease surveillance at the requisite scale for national food security monitoring (Hilton *et al.*, 2021; Mahlein, 2016; Rasti *et al.*, 2018; Zhong *et al.*, 2022).

Challenges and future work

The application of hyperspectral imaging (HSI) technology in real field environments of agriculture is facing a number of technical or practical challenges especially wheat disease detection, which has many potential applications (Behmann *et al.*, 2015; García-Vera *et al.*, 2024; Hilton *et al.*, 2021; Kamilaris and Prenafeta-Boldú, 2018; Li *et al.*, 2019; Mahlein, 2016).

- **High dimensionality:** Hyperspectral data usually have several hundreds of contiguous, very narrow spectral bands that can cause the Hughes phenomenon/the curse of dimensionality, which is known to impact classifier performance and burden the computational cost with increasing dimensions in the absence of sufficient training samples (Behmann *et al.*, 2015; Li *et al.*, 2019; Rasti *et al.*, 2018; Zhang *et al.*, 2019; Zhong *et al.*, 2022).

- **High sensor cost:** Hyperspectral cameras are still expensive, especially for smallholder farmers or if the system is to be deployed in many fields. Furthermore, there is also an additional cost in requiring a systems solution for stable calibration, high spectral fidelity and ruggedization (Hilton *et al.*, 2021; Mahlein, 2016; Rasti *et al.*, 2018).
- **Environmental variability:** Factors such as differences in illumination, canopy structure, soil reflectance and atmospheric conditions add to spectral noise and alter reflectance values leading to inconsistent disease classification under realistic field based environment (Haagsma *et al.*, 2023; Hilton *et al.*, 2021; Li *et al.*, 2019; Mahlein, 2016; Rasti *et al.*, 2018).
- **Limited labeled datasets:** To train models accurately, large annotated datasets of healthy and diseased wheat under a variety of environments at different stages need to be developed. This lack of open and standardized hyperspectral datasets is seriously hampering the scalability and transferability of machine learning-based models (Behmann *et al.*, 2015; García-Vera *et al.*, 2024; Kamilaris and Prenafeta-Boldú, 2018; Li *et al.*, 2019; Ualiyeva *et al.*, 2025; Zhong *et al.*, 2022; Gupta and Soni, 2022).

In order to manage these challenges, the research is looking at few of many interesting future directions:

- **Edge computing and iot integration:** These lightweight, energy-efficient models can be deployed on edge devices (*e.g.,* drones, field sensors) to enable real-time disease detection so that reliance on cloud-based processing is minimized and responsiveness in precision agriculture is improved (García-Vera *et al.*, 2024; Li *et al.*, 2019; Mahlein, 2016; Xu *et al.*, 2018; Zhong *et al.*, 2022).
- **Federated learning:** Federated learning as an approach to decentralized model training using data from multiple farms or regions without having to centralize the raw data and emerging solutions for privacy-preserving and scalability in hyperspectral (HS) data modeling under distributed setting, particularly when data sharing is limited (Kamilaris and Prenafeta-Boldú, 2018; Li *et al.*, 2019; Zhong *et al.*, 2022).
- **Explainable AI (XAI):** Because DL models are frequently referred to as black boxes, XAI techniques are currently being developed to explain model decisions, find important spectral bands or regions of interest (ROIs) and improve the trustworthiness of the method among agronomists and decision makers (Kamilaris and Prenafeta-Boldú, 2018; Li *et al.*, 2019; Li *et al.*, 2020; Zhong *et al.*, 2022).
- **Multisensor fusion:** Combining HSI with other modalities such as LiDAR, thermal imaging, or RGB cam eras also offers more complex data representation and increases the robustness of disease detection models to various field conditions (Chang *et al.*, 2024; García-Vera *et al.*, 2024; Li *et al.*, 2019; Mahlein, 2016; Mortensen *et al.*, 2020).

These guidelines making hyperspectral sensing more understandable, interpretable and field-deployable towards accelerated adoption in smart agriculture and early disease warning systems (García-Vera *et al.*, 2024; Kamilaris and Prenafeta-Boldú, 2018; Li *et al.*, 2019; Mahlein, 2016).

CONCLUSION

Hyperspectral imaging has proved to be an extraordinary technology for early, accurate and non-destructive diagnosis of diseases in wheat crops with the application of advanced deep learning models such as 3D-CNNs, Vision Transformers and hybrid spectral-spatial models reaching classification accuracy of up to 98% in a controlled environment. However, critical analysis of the reviewed literature shows persistent research gaps such as lack of large-scale standardized benchmark datasets, limited validation of models under real-world field conditions, underrepresentation of multi-disease co-infection scenarios and insufficient development of explainable AI frameworks, which are crucial for building agronomist trust in operational deployment. Closing these gaps will require the development of openly accessible community-standard HSI wheat disease datasets, lightweight edge-deployable architectures, fusing HSI with complementary modalities such as LiDAR and thermal imaging and the adoption of federated learning frameworks that enable geographically distributed model training without centralizing sensitive agricultural data. Recent advances in hyperspectral sensor miniaturization, deep learning model efficiency, edge computing capabilities and satellite data delivery infrastructure combine to create an unprecedented opportunity for the integration of HSI-based disease detection into routine precision wheat farming over the next decade. Turning this opportunity into reality demands sustained interdisciplinary work that integrates remote sensing, machine learning, plant pathology and agricultural engineering to achieve the shared goal of translating the technical potential of hyperspectral imaging into significant and lasting progress for global food security.

ACKNOWLEDGEMENT

The present study was supported by this research received no specific grant from any funding agency in the public, commercial, or not-for-profit sectors.

Disclaimers

The views and conclusions expressed in this article are solely those of the authors and do not necessarily represent the views of their affiliated institutions. The authors are responsible for the accuracy and completeness of the information provided, but do not accept any liability for any direct or indirect losses resulting from the use of this content.

Conflict of interest

The authors declare that there are no conflicts of interest regarding the publication of this article. No funding or sponsorship influenced the design of the study, data collection, analysis, decision to publish, or preparation of the manuscript.

REFERENCES

Abdulridha, J., Min, A., Rouse, M.N., Kianian, S., Isler, V. and Yang, C. (2023). Evaluation of stem rust disease in wheat fields by drone hyperspectral imaging. *Sensors*. **23(8):** 4154.

Audebert, N., Le Saux, B. and Lefèvre, S. (2018). Beyond RGB: Very high resolution urban remote sensing with multimodal deep networks. *ISPRS Journal of Photogrammetry and Remote Sensing*. **140:** 20-32.

Behmann, J., Steinrücken, J. and Plümer, L. (2015). A review of advanced machine learning methods for the classification of hyperspectral data in precision agriculture. *Remote Sensing*. **7(6):** 7221-7249.

Carvalho, I.C.B., Ferreira, M.E., Paiva, M.R. and Silva, G.R. (2025). Hyperspectral imaging and machine learning approach for rapid and non-invasive diagnosis of cassava bacterial blight. *Frontiers in Plant Science*. **16:** 1583291.

Chang, S., Yang, G., Cheng, J., Feng, Z., Fan, Z., Ma, X. and Zhao, C. (2024). Recognition of wheat rusts in a field environment based on improved DenseNet. *Biosystems Engineering*. **238:** 10-21.

Chossegros, M., Hubbard, A., Burt, M., Harrison, R.J., Nellist, C.F. and Grinberg, N.F. (2025). Hyperspectral image analysis for classification of multiple infections in wheat. *Plant Methods*. **21(1):** 144. doi: 10.1186/s13007-025-01461-x.

Erdilo, B.T., Vadapalli, H. and Haar, D.V.D. (2025). Enhancing crop disease detection with deep learning and hyperspectral imaging: A focus on Fusarium Head Blight. International Conference on Artificial Intelligence and Soft Computing. Springer Nature Switzerland. pp. 89-101.

Fedotov, A., Eremenko, D., Kuznetsova, D., Baranova, O. and Terentev, A. (2025). Advanced hyperspectral image processing and machine learning approaches for early detection of wheat stem rust. *Frontiers in Plant Science*. **16:** 1725017.

Feng, Y., Lu, Q., Liang, X., Perez, D., Zhou, L. and He, Y. (2020). Early detection of wheat stripe rust using UAV-based hyperspectral imagery. *Sensors*. **20(18):** 5125.

Feng, Z.H., Wang, L.Y., Yang, Z.Q., Zhang, Y.Y., Li, X., Song, L. and Feng, W. (2022). Hyperspectral monitoring of powdery mildew disease severity in wheat based on machine learning. *Frontiers in Plant Science*. **13:** 828454.

García-Vera, Y.E., Polochè-Arango, A., Mendivelso-Fajardo, C.A. and Gutiérrez-Bernal, F.J. (2024). Hyperspectral image analysis and machine learning techniques for crop disease detection and identification: A review. *Sustainability*. **16(14):** 6064.

Gogoi, N.K., Deka, B. and Bora, L.C. (2018). Remote sensing and its use in detection and monitoring plant diseases: A review. *Agricultural Reviews*. **39(4):** 307-313. doi: 10.18805/ag.R-1835.

Goyal, S.B., Malik, V., Rajawat, A.S., Khan, M., Ikram, A., Alabdullah, B. and Almjally, A. (2025). Smart intercropping system to detect leaf disease using hyperspectral imaging and hybrid deep learning for precision agriculture. *Frontiers in Plant Science*. **16:** 1662251.

Guo, D., Zhang, L., Liu, X. and Li, J. (2019). Hyperspectral image classification using a context-sensitive deep CNN model. *IEEE Access*. **7:** 100375-100385.

Gupta, A.K. and Soni, P. (2022). Wheat crop yield estimation using geomatics tools in Saharanpur District. *Indian Journal of Agricultural Research*. **56(5):** 519-526. doi: 10.18805/IJARe.A-5331.

Haagsma, M., Hagerty, C.H., Kroese, D.R. and Selker, J.S. (2023). Detection of soil-borne wheat mosaic virus using hyperspectral imaging: From lab to field scans and from hyperspectral to multispectral data. *Precision Agriculture*. **24(3):** 1030-1048.

Hang, R., Liu, Q., Hong, D. and Ghamisi, P. (2019). Classification of hyperspectral images with capsule networks. *IEEE Geoscience and Remote Sensing Letters*. **16(11):** 1650-1654.

Hilton, A.J.W., Jennings, P., Hollins, T.W. and Conner, R.L. (2021). Spectral imaging in agriculture: An overview of hardware, techniques and applications. *Biosystems Engineering*. **204:** 1-20.

Kamilaris, A. and Prenafeta-Boldú, F.X. (2018). Deep learning in agriculture: A survey. *Computers and Electronics in Agriculture*. **147:** 70-90.

Khan, M.A., Asif, M., Ahmad, S. and Ullah, I. (2021). A novel deep learning framework for automated diagnosis of wheat diseases using hyperspectral data. *Agronomy*. **11(3):** 498.

Krizhevsky, A., Sutskever, I. and Hinton, G.E. (2012). ImageNet classification with deep convolutional neural networks. *Advances in Neural Information Processing Systems*. **25:** 1097-1105.

Li, S., Song, W., Fang, L., Chen, Y., Ghamisi, P. and Benediktsson, J.A. (2019). Deep learning for hyperspectral image classification: An overview. *IEEE Transactions on Geoscience and Remote Sensing*. **57(9):** 6690-6709.

Li, Z., Huang, L., Zhang, J. and Zhao, J. (2020). Spectral-spatial residual network with spatial-spectral attention mechanism for hyperspectral image classification. *Remote Sensing*. **12(9):** 1481.

Mahlein, A.K. (2016). Plant disease detection by imaging sensors -parallels and specific demands for precision agriculture and plant phenotyping. *Plant Disease*. **100(2):** 241-251.

Metagar, S.M. and Walikar, G.A. (2024). Machine learning models for plant disease prediction and detection: A review. *Agricultural Science Digest*. **44(4):** 591-602. doi: 10.18805/ag.D-5893.

Mortensen, A.K., Lillemo, M. and Muath, A. (2020). UAV-based hyperspectral and thermal imagery for early detection of diseases in wheat. *Precision Agriculture*. **21:** 1009-1025.

Rasti, B., Hong, D., Hang, R., Ghamisi, P., Kang, X., Chanussot, J. and Benediktsson, J.A. (2018). Feature extraction for hyperspectral image classification: A review. *IEEE Geoscience and Remote Sensing Magazine*. **6(3):** 44-76.

Terentev, A., Badenko, V., Shaydayuk, E., Emelyanov, D., Eremenko, D., Klabukov, D. and Dolzhenko, V. (2023). Hyperspectral remote sensing for early detection of wheat leaf rust caused by *Puccinia triticina*. *Agriculture*. **13(6):** 1186.

Ualiyeva, R.M., Kaverina, M.M., Osipova, A.V., Kairbayev, Y.B., Zhangazin, S.B., Iksat, N.N. and Mapitov, N.B. (2025). VNIR hyperspectral signatures for early detection and machine-learning classification of wheat diseases. *Plants*. **14(23):** 3644.

Wahabzada, M., Mahlein, A.K., Bauckhage, C., Steiner, U., Oerke, E.C. and Kersting, K. (2016). Plant phenotyping using probabilistic topic models: Uncovering the hyperspectral language of plants. *Scientific Reports*. **6(1):** 22482.

Wang, Q., Li, Q. and Li, X. (2019). Spectral-spatial feature extraction based on deep learning for classification of hyperspectral images. *Remote Sensing*. **11(9):** 1070.

Xie, Y., Han, L., Liu, H. and Shi, Y. (2017). Hyperspectral imaging for early detection of wheat stripe rust. *Remote Sensing*. **9(5):** 422.

Xu, Y., Du, B., Zhang, L. and Zhang, F. (2018). Multiscale 3D deep convolutional neural network for hyperspectral image classification. *IEEE Transactions on Geoscience and Remote Sensing*. **56(8):** 4426-4441.

Zhang, W., Li, A., Jiang, N. and Li, J. (2019). Data fusion approaches for hyperspectral image classification: A review. *IEEE Geoscience and Remote Sensing Magazine*. **7(2):** 97-119.

Zhang, Y., Cao, G., Li, X. and Wang, B. (2016). Spectral-spatial classification of hyperspectral images using deep convolutional neural networks. *Remote Sensing Letters*. **7(9):** 747-756.

Zhong, S., Chang, C., Zhang, L. and Li, J. (2022). Spectral-spatial residual network for hyperspectral image classification: A 3D deep learning framework. *IEEE Transactions on Geoscience and Remote Sensing*. **60:** 1-14.

Zhu, J., Yang, G., Feng, X., Li, X., Fang, H., Zhang, J., Bai, X., Tao, M. and He, Y. (2022). Detecting wheat heads from UAV low-altitude remote sensing images using deep learning based on Transformer. *Remote Sensing*. **14(20):** 5141.